A Fast MAP Algorithm for 3D Ultrasound

João M. Sanches* Jorge S. Marques

IST/ISR, Torre Norte, Av. Rovisco Pais, 1049-001, Lisbon, Portugal

Abstract. Bayesian methods have been avoided in 3D ultrasound. The multiplicative type of noise which corrupts ultrasound images leads to slow reconstruction procedures if Bayesian principles are used. Heuristic approaches have been used instead in practical applications.

This paper tries to overcome this difficulty by proposing an algorithm which is derived from sound theoretical principles and fast. This algorithm is based on the expansion of the noise probability density function as a Taylor series, un the vicinity of the maximum likelihood estimates, leading to a linear set of equations which are easily solved by standard techniques. Reconstruction examples with synthetic and medical data are provided to evaluate the proposed algorithm.

* please send all the correspondence to Joao Sanches, ISR, Torre Norte, Av. Rovisco Pais, 1049-001 Lisboa, Portugal, Email:jmrs@alfa.ist.utl.pt, Phone:+351 21 8418195

1 Introduction

This paper addresses the problem of 3D ultrasound. 3D ultrasound aims to reconstruct the human anatomy from a set of ultrasound images, corresponding to cross-sections of the human body. Based on this information, the idea is to estimate a volume of interest for diagnosis proposes. This technique is wide spread due essentially to its non invasive and non ionizing characteristics [1]. Furthermore, the ultrasound equipment is less expensive than other medical modalities, such CT, MRI or PET [2,3]. One way to perform 3D ultrasound is by using 2D ultrasound equipment with a spatial locator attached to the ultrasound probe, giving the position and orientation of the cross-section along the time(see Fig.1). The estimation algorithm should fuse these information, image and position, to estimate the volume.

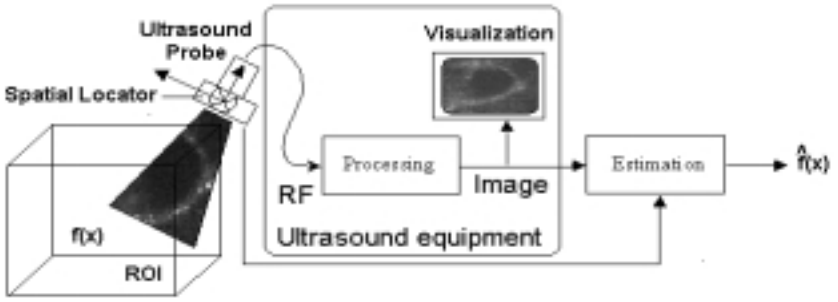

Fig. 1. 3D ultrasound acquisition system

Traditionally ultrasound imaging technique is made in real time using the B-scan mode. The inspections results are visualized in real time being allowed to the medical doctor to choose the best cross sections for the diagnosis. In 3D ultrasound this goal is much more difficult to achieve since the amount of data is much higher. However, reconstruction time should be kept as small as possible. This is the reason why a lot of algorithms used in 3D ultrasound are designed in ad hoc basis [4,5], aiming to be as simple and fast as possible.

Bayesian approaches in 3D ultrasound have been avoided since these methods are usually computationally demanding. In this paper we present an algorithm for 3D ultrasound designed in a Bayesian framework. Its theoretical foundation is presented as well the simplification procedures and justifications in order to speed up the reconstruction process. Our goal is to designed an efficient reconstruction algorithm to work in a quasi real time basis, while keeping a solid theoretical foundation.

This paper is organized as follows. Section 2 describes the problem of 3D reconstruction and the notation adopted in this paper. Sections 3 and 4 present two algorithms for 3D reconstruction: the standard solution and a fast algorithm.

Section 5 present experimental results with synthetic and real data using both algorithms. Finally section 6 concludes the paper.

2 Problem Formulation

This section describes the reconstruction of a 3D function f from a set of ultrasound images. Additional details can be found in [6].

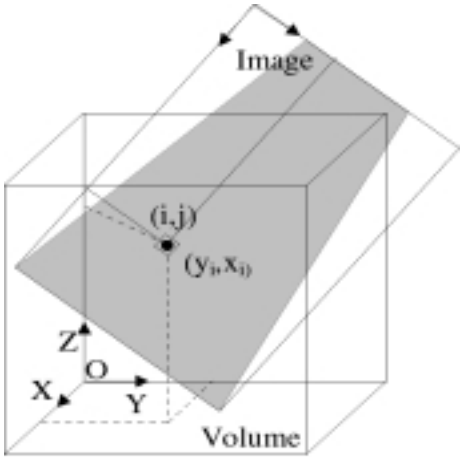

Fig. 2. Volume and image coordinates

Let us consider a scalar function $f(x)$ defined in $\Omega \subset R^3$, i.e., $f : \Omega \rightarrow R$. We assume that this function is expressed as a linear combination of known basis functions, i.e.,

$$f(x) = \sum_g b_g(x) u_g \tag{1}$$

where $u_1, u_2, ..., u_N$ are the unknown coefficients to be estimated and $b(x_i)$ are known basis functions centered at the nodes of a 3D regular grid. Let $\{y_i\}$ be a set of intensity data points, measuring $f(x)$ at locations $\{x_i\}$, belonging to one of the inspection planes. It is assumed that intensity measurements, y_i, are corrupted by multiplicative noise and the goal is to estimate $f(x)$ based on the observations $\{y_i\}$.

This estimation problem can be formulated in a Bayesian framework using a MAP criterion, as follows: given a set of data $Y = \{y_i\}$ with a distribution $p(Y|U)$ which depends on the unknown parameters, $U = \{u_g\}$ with a prior distribution $p(U)$, estimate U in order to maximize the joint probability density function of the data and parameters, $p(Y, U)$, i.e.,

$$\hat{U} = arg \max_U \log(p(Y|U)p(U)) \tag{2}$$

In this paper we assume that all the elements of Y are i.i.d. (independent and identically distributed) [8] with a Rayleigh distribution [9], i.e.,

$$\log p(Y|U) = \sum_i \{\log(\frac{y_i}{f(x_i)}) - \frac{y_i^2}{2f(x_i)}\} \tag{3}$$

where $f(x_i)$ is the value of the function to be reconstructed f at x_i.

The prior used is gaussian [10], i.e.,

$$p(U) = \frac{1}{Z} e^{-\psi \sum_g \sum_i (u_g - u_{gi})^2} \tag{4}$$

where u_{gi} is a neighbor of u_g and Z is a normalization factor.

Therefore, the objective function can be expressed as

$$L(U) = l(U) + q(U) \tag{5}$$

where $l = \log p(Y/U)$ is the log likelihood function of the data and $q = \log p(U)$ is the logarithm of the prior associated to the unknown parameters.

To optimize (5) the ICM algorithm proposed by Besag [7] is used. The ICM algorithm simplifies the optimization process by optimizing the objective function with respect to a single variable at a time, keeping the other variables constant. Each step is a 1D optimization problem which can be solved in a number of ways. This step is repeated for all the unknown coefficients in each iteration of the ICM algorithm.

To optimize (5) with respect to a single coefficient u_p the stationary equation,

$$\frac{\partial l(U)}{\partial u_p} + \frac{\partial q(U)}{\partial u_p} = 0 \tag{6}$$

is numerically solved.

The next sections present two approaches to compute (6). Section 3 attempts to solve this equation using nonlinear optimization methods. Section 4 presents a fast algorithm based on the solution of a linear set of equations. The second perform some simplifications in order to speed up the computations. Both methods are iterative.

3 Nonlinear method

Let us first compute the derivatives of l and q.

After straightforward manipulation it can be concluded that

$$\frac{\partial l(U)}{\partial u_p} = \frac{1}{2} \sum_i (\frac{y_i^2 - 2f(x_i)}{f(x_i)^2} b_p(x_1)) \tag{7}$$

where the sum is performed for all data points that are in the neighborhood $[-\Delta, \Delta]^3$ of the p-th node. In fact, each data point contributes to the estimation of its 8 neighboring coefficients (see Fig.3).

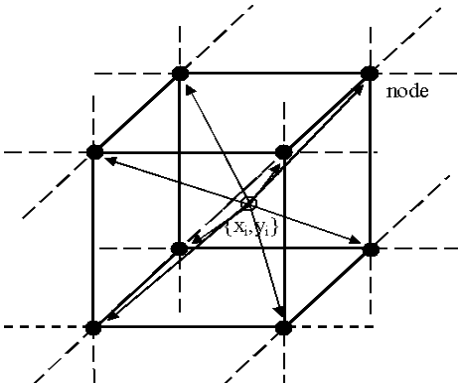

Fig. 3. Neighboring nodes of a data point.

It is also easy to concluded that

$$\frac{\partial q(U)}{\partial u_p} = -2\psi N_v(u_p - \bar{u}_p) \tag{8}$$

where N_v is the number of neighbors of u_p ($N_v = 6$) and $\bar{u}_p$ is the average intensity computed using the N_v neighbors.

To optimize the objective function a set of non-linear equations should be solved,

$$\frac{1}{2}\sum_i \left(\frac{y_i^2 - 2f(x_i)}{f(x_i)^2} b_p(x_1)\right) - 2\psi N_v(u_p - \bar{u}_p) = 0 \tag{9}$$

This is an huge optimization problem, which must be solved using numerical methods. The ICM algorithm proposed by Besag [7] is used and each equation is numerically solved by using the Newton-Rapson method assuming that the other coefficients, $u_k, k \neq p$ are known. The computation of the solution of (9) is computationally heavy, presenting some undesirable difficulties.

First, it would be nice to factorize the equation in two terms, one depending only on the data and the other depending on the unknown to estimate,

$$h(u_p)g_1(Y)r_1(U \setminus \{u_p\}) + g_2(Y)r_2(U \setminus \{u_p\}) + C = 0 \tag{10}$$

where $g_1(Y)$ and $g_2(Y)$ are sufficient statistics. This formulation would allow to concentrate the influence of the observed data on a small set of coefficients, computed once for all at the first iteration and kept unchanged during the optimization process. Data processing would be done only once speeding up the estimation process.

Unfortunately, it is not possible to write (9) in the form of (10), i.e., there are no sufficient statistics for the estimation of the interpolating function f. This means that all the data must be read from the disk and processed in each iteration of the nonlinear reconstruction algorithm. This is a strong limitation

when a large number of cross-sections is involved, e.g., 1000 images with 640×480 pixels will lead to $3072e5$ pixels, preventing a wide spread use of this algorithm.

Another important difficulty concerns the stability of the convergence process. The system of equations (9) is non-linear. The stability of the numerical methods used to solve it, strongly depends on the data and on the regularization parameter, ψ, and on the initial estimates of U. The process of finding the right parameters to obtain acceptable reconstructions is in general often done by trial and error.

To overcome these difficulties an approximation approach is proposed in the next section.

4 Linear solution

Let us develop $l(U)$ in Taylor series about the maximum likelihood estimates, U_{ML},

$$l(u_p) = l(u_p^{ML}) + \frac{\partial l(u_p^{ML})}{\partial u_p}(u_p - u_p^{ML}) + \frac{1}{2}\frac{\partial^2 l(u_p^{ML})}{\partial u_p^2}(u_p - u_p^{ML})^2 + \epsilon \qquad (11)$$

the first derivative of $l(U)$ with respect to u_p is

$$\frac{\partial l(U)}{\partial u_p} \approx \frac{\partial^2 l(u_p^{ML})}{\partial u_p^2}(u_p - u_p^{ML}) \qquad (12)$$

where it was assumed that $\frac{\partial l(u_p^{ML})}{\partial u_p} = 0$ since by definition U_{ML} is a stationary point of $l(U)$. The residue ϵ was discarded for convenience.

Thus (6) takes the form

$$\frac{\partial L(U)}{\partial u_p} \approx \frac{\partial^2 l(u_p^{ML})}{\partial u_p^2}(u_p - u_p^{ML}) - 2\psi N_v(u_p - \bar{u}_p) = 0 \qquad (13)$$

leading to

$$u_p = \frac{1}{1+\tau_p}u_p^{ML} + \frac{\tau_p}{1+\tau_p}\bar{u}_p \qquad (14)$$

where $\tau_p = -\frac{2\psi N_v}{\partial^2 l(u_p^{ML})\backslash \partial u_p^2}$

Equations show that the MAP estimation can be seen as a linear combination of the ML estimates with the average intensity computed in the neighborhood of each node.

Let us compute the maximum likelihood estimation of U.

Assuming that $f(x)$ changes slowly in the neighborhood of each node, i.e., $f(x_i) \approx u_p$ will be used in (7) to obtain

$$\frac{\partial l(U)}{\partial u_p} = \frac{1}{2u_p^2}\sum_i (y_i^2 b_p(x_i)) - \frac{1}{u_p}\sum_i (b_p(x_i)) = 0 \qquad (15)$$

Solving with respect to u_p^{ML} leads to

$$u_p^{ML} = \frac{1}{2}\frac{\sum_i (y_i^2 b_p(x_i))}{\sum_i b_p(x_i)} \tag{16}$$

and by deriving (15) in order to u_p leads to

$$\frac{\partial^2 l(u_p^{ML})}{\partial u_p^2} = -\frac{\sum_i b_p(x_i)}{(u_p^{ML})^2} \tag{17}$$

This expression for the second derivative of the log likelihood function, obtained by deriving (15) with respect to u_p, can be more accurately computed if (7) is used. By deriving two times (7) with respect to u_p and after replacing $f(x_i)$ by u_p it obtains:

$$\frac{\partial^2 l(u_p^{ML})}{\partial u_p^2} = -\frac{\sum (y_i b_p(x_i))^2}{(u_p^{ML})^3} + \frac{\sum b_p^2(x_i)}{(u_p^{ML})^2} \tag{18}$$

We have used expression (17) in the reconstruction using synthetic data and (18) in the case of real data.

Therefore, the MAP estimate of the volume of interest is obtained by solving a system of linear equations given by (14) where $\tau_p = \frac{2\psi N_v}{\sum_i b_p(x_i))}(u_p^{ML})^2$ and where u_p^{ML} is given by(16).

For sake of simplicity (14) can be rewrite as

$$u_p = k_p + c_p \bar{u}_p \tag{19}$$

where $k_p = \frac{u_p^{ML}}{1+\tau_p}$ and $c_p = \frac{\tau_p}{1+\tau_p}$. These parameters, k_p and c_p are computed once for all during the initialization phase. The solution of (14) can be done by standard algorithms for the solution of linear sets of equations.

5 Experimental Results

This section presents two 3D reconstruction examples using synthetic and real data.

The synthetic data consists of a set of 100 images of 128×128 pixels corresponding to parallel cross sections of the 3D interval $[-1,1]^3$ (see Fig.4). The function to be reconstructed is assumed to be binary: $f(x) = 5000, x \in [-0.5, 0.5]^3, f(x) = 2500$ otherwise. The cross sections were corrupted with Rayleigh noise according to (3). The histogram of the whole set of images is shown in Fig.5 and is a mixture of two Rayleigh densities. Both reconstruction algorithm were used to reconstruct f in the interval $[-1,1]^3$ using a regularization parameter $\psi = 16.10^{-6}$.

Fig.6 shows the profiles extracted from the estimated volumes using both methods. These two profiles are quite similar which means that both methods

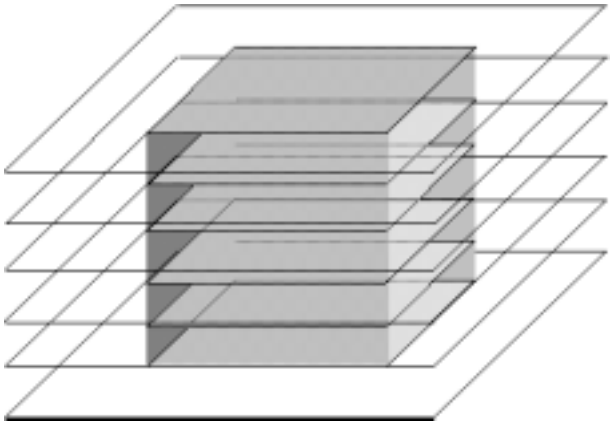

Fig. 4. Cross sections extracted from a synthetic 3D cube

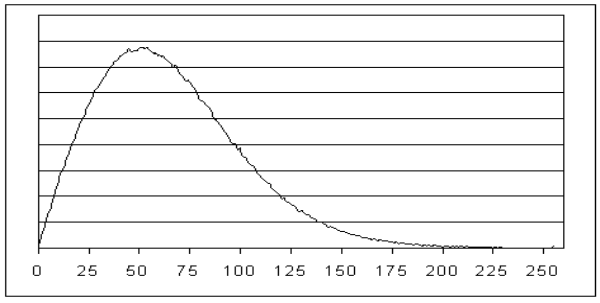

Fig. 5. Synthetic data set histogram

lead to similar results in this problem. The SNR of 21.4dB for the nonlinear method and 20.8dB for the fast algorithm proposed in this paper stresses the ability of the linear algorithm to produce similar results as those obtained with the nonlinear method.

It should be stressed that the linear method is less heavy in computational terms. Fig.7 and Fig.8 show the evolution of the posteriori distribution function, $\log(p(Y,U))$ along the iterative process. Fig.7 displays $\log(p(Y,U))$ as function of the index of the iteration while Fig.8 displays the same values as function of the time.

The nonlinear algorithm converges in less iterations(62) than the linear algorithm(97) in this example. However, since each iteration of the nonlinear method is slower and it involves processing all (millions) of the observations, the convergence is slower in terms of computation time (see Fig.8) (in this case about 6 times slower than the linear method [1]).

Fig. 9 shows cross sections of the 3D volume (left) as well as the 3D surface of the cube displayed using rendering methods (right). The results are again similar, the nonlinear method performing slightly better at the transitions.

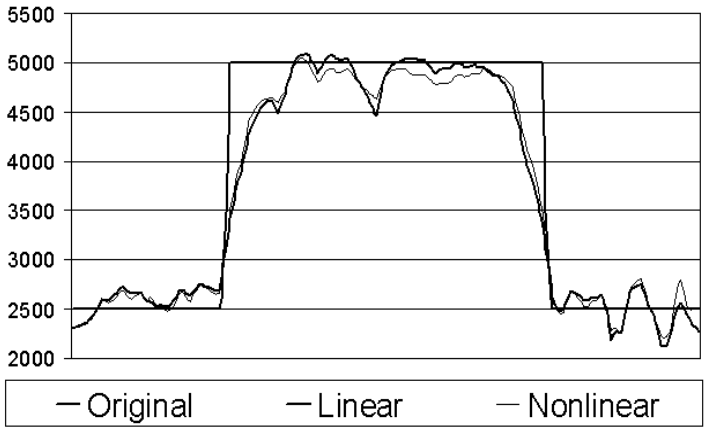

Fig. 6. Profiles extracted from the original volume and from the estimated volumes using the nonlinear and linear methods

The real data if formed by a set of 100 images of a human thyroid with 128×128 pixels. Fig.10 shows the corresponding histogram. This histogram reveals some significant differences from the one of the synthetic data. In the case of the synthetic data the underlying 3D object is binary while in the case of the real data a continuous range of reflectivity values are admissible.

[1] These values depend on the number and dimensions of the images and on the desired accuracy for the solution. For very accurate solutions it is need more iterations and the linear method becomes more efficient

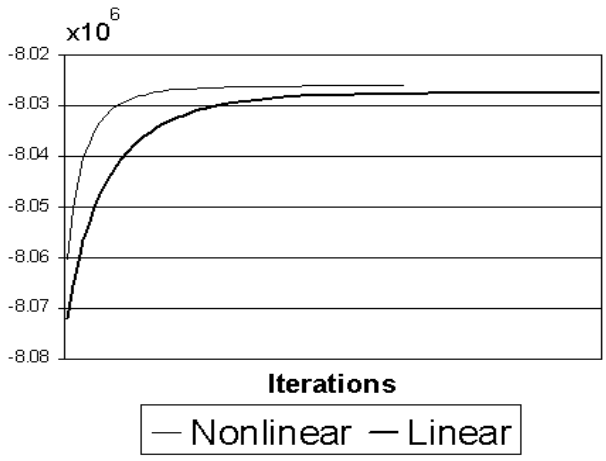

Fig. 7. L(U) along the iterative process

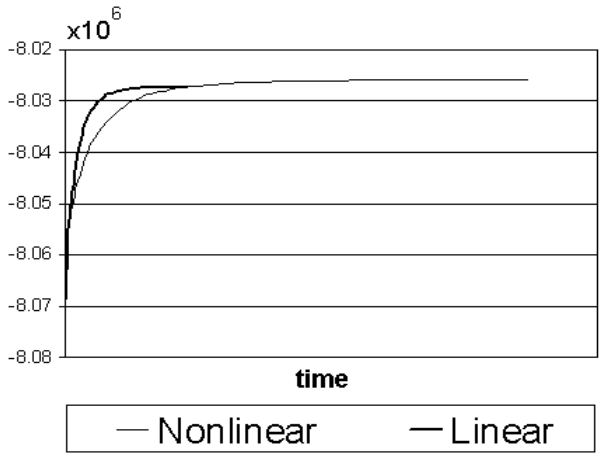

Fig. 8. L(U) along the iterative process in function of time

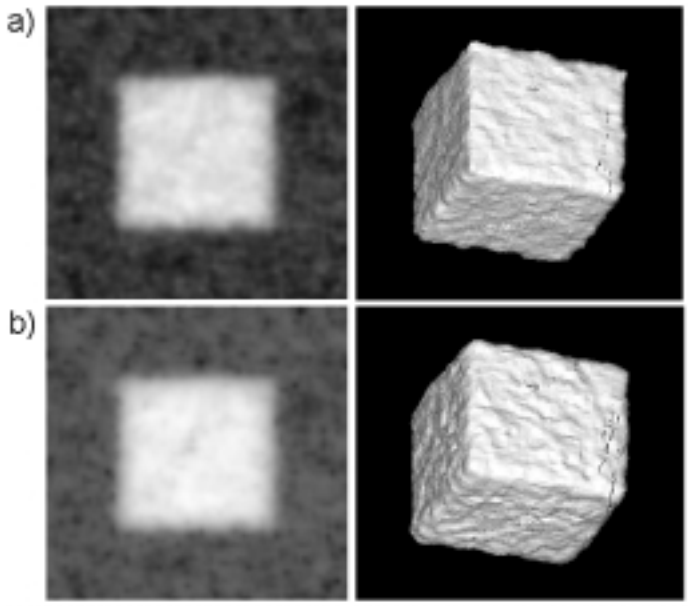

Fig. 9. Reconstructed volumes, a)using the nonlinear method and b) using the linear method

Profiles extracted from both estimated volumes are shown in Fig.11. In this figure are also shown images belonging to the initial data set. The profiles were computed from images extracted from the estimated volumes with dimensions and positions equivalent to the cross-sections shown in the figure. In this graph it is also shown a profile extracted from a maximum likelihood estimates computed by using the expression (16). Here, the difference between both methods are more visible which is related with the deviation of the real data from the true Rayleigh model. However, we conclude once more that the linear method leads to acceptable results, similar to the ones obtained with the nonlinear algorithm.

6 Conclusion

This paper presents an algorithm to estimate the acoustic reflectivity in a given region of interest from a set of ultrasound images. The images are complemented with the position and orientation of the ultrasound probe. The proposed algorithm is formulated in a Bayesian framework using a MAP criterion. To speed the reconstruction time a simplified (linear) algorithm was proposed based on the concept of sufficient statistics.

The goal is obtain a fast and efficient MAP algorithm to estimate volumes in a quasi real time basis. Reconstruction results obtained with both methods are presented, one using a set of images extracted from a synthetic 3D cube and the other using a set of real cross-sections of a human thyroid. Both examples

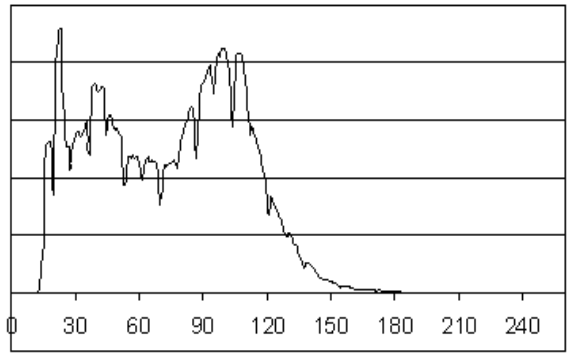

Fig. 10. Real data histogram

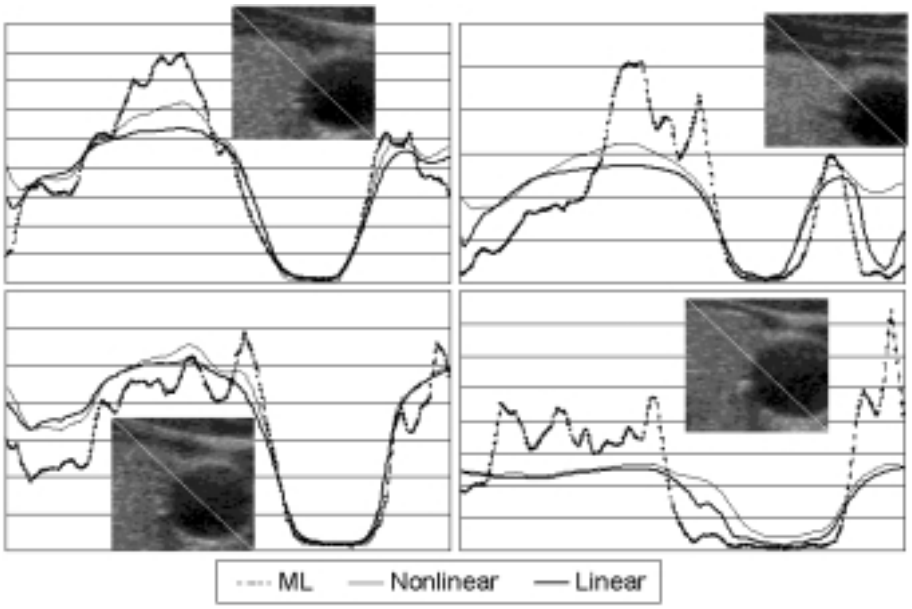

Fig. 11. Profiles extracted from the estimated volumes using the nonlinear and linear method

show that the fast(linear) algorithm performs almost as well as the nonlinear version. Profiles extracted from the estimated volumes are quite similar and the signal to noise ration (for the synthetic case only) computed with the original volume reenforce this similarity. It is concluded that the linear algorithm needs more iterations to reconstruct the volume than the nonlinear one but it spend mutch less time. This is explained by the fact that the linear method only has to process the huge amount of data only once, while the nonlinear method must read and process the data in each iteration. A final note should be provide. The formulation of the linear method is more simple than the nonlinear method. The estimation process in the first case is obtained by solving a set of linear equations while in the non simplified case a set of non-linear equations should be solved. The nonlinear method present problems of convergence and stability, that are not addressed in this paper, which are also solved by using the linear reconstruction method proposed in this paper.

References

1. T. Nelson, D. Downey, D. Pretorius, A. Fenster, Three-Dimensional Ultrasound, Lippincott, 1999.
2. J. Quistgaard, Signal Acquisition and Processing in Medical Diagnostics Ultrasound, IEEE Signal Processing Magazine, vol.14, no.1, pp 67-74, January 1997.
3. G.T.Herman, A.Kuba, Discrete Tomography, Foundations, Algorithms, and Applications, Birkhauser, 1999.
4. R.N.Rohling, A. H. Gee and L. Berman, A comparation of freehand three-dimensional ultrasound reconstruction techniques, Medical Image Analysis, vol.4, no.4, pp.339-359, 1999.
5. S. Ogawa et al., Three Dimension Ultrasonic Imaging for Diagnosis of Beast Tumor,Ultrasonics Symp., 1998.
6. J. Sanches, J.Marques, A Rayleigh reconstruction/interpolation algorithm for 3D ultrasound, Pattern Recognition Letters, 21, pp. 917-926, 2000.
7. J. Besag, On the Statistical Analysis of Dirty Pictures, J. R. Statist. Soc. B, vol.48, no. 3, pp. 259-302, 1986.
8. J. Dias and J. Leitão, Wall position and thickness estimation from sequences of echocardiograms images, IEEE Transactions on Medical Imaging, vol.15, pp.25-38, February 1996.
9. C. Burckhardt, Speckle in Ultrasound B-Mode Scans, IEEE Trans. on Sonics and Ultrsonics, vol. SU-25, no.1, pp.1-6, January 1978.
10. S.Z.Li, Close-Form Solution and Parameter Selection for Convex Minimization-Based Edge-Preserving Smoothing, IEEE Trans. on PAMI, vol. PAMI-20, no.9, pp.916-932, September 1998.